IEEE Access
Multidisciplinary | Rapid Review | Open Access Journal

SPECIAL SECTION ON INTELLIGENT BIG DATA ANALYTICS FOR INTERNET OF THINGS, SERVICES AND PEOPLE

Received June 16, 2021, accepted July 26, 2021, date of publication August 2, 2021, date of current version October 15, 2021.

Digital Object Identifier 10.1109/ACCESS.2021.3101909

Implementation of Universal Health Management and Monitoring System in Resource-Constrained Environment Based on Internet of Things

MIN ZHENG AND SHIZHEN BAI
School of Business, Harbin University of Commerce, Harbin 150028, China
Corresponding author: Min Zheng (zhengmin0532@163.com)

ABSTRACT The physiological health and chronic diseases of humans can be monitored by linking up health management and monitoring (HMM) system with the Internet of things (IoT), which transcends the restrictions of time and space. However, the IoT network faces several resource constraints, such as limited storage and initial energy of nodes, long delay of response to system transmission, and low rate of successful payments. To solve these problems, this paper explores the IoT-based implementation of universal HMM system in resource-constrained environment. Firstly, the forwarding utility of the communication between adjacent IoT nodes was estimated, and an incentive strategy was prepared for the IoT nodes in the resource-constrained environment. Next, a universal HMM system was designed, and the scheme for denoising, baseline drift filtering, and feature point detection was introduced step by step. After that, the authors presented the design process of the communication protocol, and the workflow of the cloud server. Through experiments, the measurements of the detection modules in the proposed universal HMM system were proved effective, and our algorithm was confirmed superior in the success rate of message delivery, the mean residual energy of nodes, and the delay of system response.

INDEX TERMS Internet of Things (IoT) network, universal health management and monitoring (HMM) system, resource-constrained environment.

I. INTRODUCTION

With the rapid progress of economy and society, people are attaching greater importance to their health conditions. Meanwhile, the Internet of things (IoT) has gained popularity, owing to the fast development of communication technology [1]–[4]. The physiological health and chronic diseases of humans can be monitored by linking up health management and monitoring (HMM) system with the IoT, which transcends the restrictions of time and space [5]–[8]. However, the application and implementation of the universal HMM system are severely challenged by the resource constraints of the IoT network, namely, limited storage and initial energy of nodes, long delay of response to system transmission, and low rate of successful payments [9]–[13].

To build an energy-efficient campus, Medrano-Gil *et al.* [14] applied the IoT technology to the design of campus energy consumption monitoring system. The terminal and topology of the system were constructed based on wireless monitoring terminal and ZigBee wireless network. The Web end of the system was developed based on browser/server (B/S) architecture and model-view-controller (VMC) pattern. The designed system realizes such function as energy consumption monitoring, management, and analysis. Feng *et al.* [15] summarized the following defects of the existing fire monitoring system: the facilities are not well monitored, the monitoring is inefficient, the historical data are not thoroughly mined, and the future trend is not predicted accurately. To make up for these defects, the ubiquitous network and IoT techniques were applied to fire monitoring system. The ubiquitous network was adopted to collect, transmit, and preprocess fire data. Then, the data were further analyzed, combined, and mined by big data algorithm. In this way, Feng *et al.* realized unified monitoring and management of various fire water resources, key monitoring areas, and fire-fighting equipment. For accurate evaluation of water quality and forecast of water quality changes in rural areas, Mitrpanont *et al.* [16] designed a four-layer architecture of smart water monitoring network, including a perception layer, a transmission layer, a processing layer, and an application

The associate editor coordinating the review of this manuscript and approving it for publication was Yuan Tian.

layer. The designed system is a low-delay, large-bandwidth, expansible, and moveable distributed system.

Based on the number of iterations of performance evaluation, Saelens *et al.* [17] constructed a wireless sensor network (WSN) for water environment monitoring, effectively extracted the performance indices, and created a medium- to long-term water quality prediction model, which couples the data fusion of recursive least squares (RLS) method and long short-term memory (LSTM) neural network. Their model can accurately forecast eight parameters of drinking water quality. To control chronic diseases that are hard to cure and easy to recur, Vicini *et al.* [18] designed a chronic disease monitoring platform, which contains a physiological health signal acquisition module, a wireless communication module, and a data cloud processing and storage module. The platform can calculate and analyze the oscillations of a series of physiological indices, such as heart rate, blood pressure, breathing, blood oxygen saturation, and blood glucose. To improve the control of patient conditions, Qiang *et al.* [19] combined naïve Bayes (NB)-IoT with cloud platform into a home health monitoring system, which encompasses a data acquisition terminal, an online transmission module, a data processing module, the OneNet cloud platform, and a personal computer (PC) end for app management. The system has several advantages, namely, wide coverage, low power consumption, and low cost. It is capable of tracking the motion trajectory, recording the real-time data on basic physiological health conditions, and issuing alarms of tripping.

In the context of industrial intelligence manufacturing, the maintenance of industrial production equipment has become extraordinarily difficult, owing to the changing working environment, complex principles and operation processes, and demand for high stability [20]–[23]. Marques and Pitarma [24] optimized the neural network model with genetic algorithm (GA) to predict the failure of industrial production equipment, achieved the collection, transmission, storage, and processing of the monitoring data on industrial production equipment based on industrial IoT (IIoT), provided detailed designs of software and hardware, and completed the full-scale test on the monitoring platform.

Overall, the existing studies on IoT application in human health management mainly concentrate on the communication connections between IoT modules and cloud server, the simplification of human data acquisition terminal, and the functional update of wireless sensors for data acquisition. Nevertheless, little attention has been paid to the message transmission of IoT nodes under resource-constrained environment. The future of our world is the connection between all things. However, the IoT is prone to network attacks, owing to the limited computing resources. To prevent the attacks, this paper discusses the implementation of a universal HMM based on the IoT in resource-constrained environment. The main contents cover the following aspects: (1) combing through and summarizing the existing research results; (2) giving an incentive strategy for system IoT nodes in resource-constrained environment based on the resources

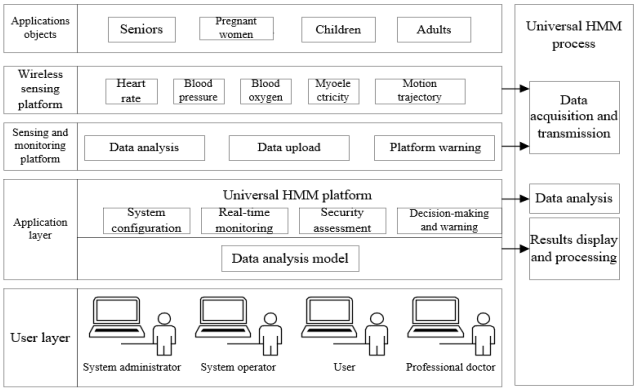

FIGURE 1. Structure of universal HMM system.

and attributes of IoT nodes, transaction rules, and message forwarding, and estimating the forwarding utility of the communication between adjacent IoT nodes; (3) designing a universal HMM system, providing the methods for denoising, baseline drift filtering, and feature point detection, and setting up the communication protocol and the workflow of the cloud server; (4) testing the measurements of the detection modules in the proposed universal HMM system, and demonstrating the superiority of our algorithm in the success rate of message delivery, the mean residual energy of nodes, and the delay of system response.

This paper combines the IoT and universal health management into the monitoring plan, and designs an IoT-based universal HMM under resource-constrained environment. The proposed plan is more reasonable than the current universal HMM plans, as indicated by a survey on existing plans and a comparison against domestic and foreign plans. Our plan helps to detect chronic diseases of humans early on, prewarn the serious illness and deterioration accurately and reliably, and improve the completeness and availability of universal health management equipment. Drawing on the thinking of IoT Plus, our plan can also enhance the quality and expertise of doctors and other health management practitioners, with the aid of information technology.

II. INCENTIVE STRATEGY FOR IoT NODES IN RESOURCE-CONSTRAINED ENVIRONMENT

A. ESTIMATION OF FORWARDING UTILITY

Figure 1 shows the structure of the proposed universal HMM system. The system monitors a diversity of scattered objects. The monitoring terminal mostly connects wireless public networks and the nearest base station to transmit the monitoring information. As a result, the continuous HMM signals are often interrupted, causing anomalies to the network. Inspired by the delay tolerant network, the opportunistic network is a self-organizing network that realizes the communication between IoT nodes, based on the store-carry-forward routing model. It is capable of transmitting signals, even if there is no complete link between sending and target nodes. Thus, the network can meet the communication demand and support the access of universal HMM system under limited resources,

and mitigate the divided state and time delay of that system. Sensitive medical data involve security and privacy issues. To handle these issues, our system is supported by a perfect discovery algorithm to pinpoint the sensitive IoT data, and is combined with decision warning and threat information processing to monitor abnormal accesses/operations of medical data. The positioning and monitoring enable the system to prevent data leakage.

In the opportunistic network, the IoT nodes all have limited resources. Under such a resource-constrained environment, every IoT node often refuse to assist other IoT nodes for free in completing message forwarding task, in order to save its own resources. To enhance the efficiency of data transmission, it is necessary to effectively detect this selfish behavior of the IoT nodes, and properly incentivize cooperation between them. This paper adopts the single-copy routing algorithm to design an incentive strategy for selfish nodes. The strategy was designed under three assumptions: the nodes have limited cache space and energy; the IoT nodes in the network are selfish; each node treats the cached messages fairly.

In the universal HMM system, an opportunistic network can be modeled as a directed graph (*ES*, *DS*), where *ES* and *DS* are the vertex set of all IoT nodes, and the edge set of all the edges linking up these nodes. To compute the forwarding utility between two IoT nodes, the first step is to calculate the mean connection duration $h^*_{C-(i,j)}$ and mean disconnection duration $h^*_{D-(i,j)}$ of the edge between nodes i and j in time window H:

$$\begin{cases} h^*_{C-(i,j)} = \sum_{l=1}^{N_M(i,j)} \dfrac{h^l_{E-(i,j)} - h^l_{S-(i,j)}}{N_M(i,j)} \\ h^*_{D-(i,j)} = \sum_{l=1}^{N_M(i,j)} \dfrac{h^{l+1}_{S-(i,j)} - h^l_{E-(i,j)}}{N_M(i,j)} \end{cases} \tag{1}$$

where, $N_{M(i,j)}$ is the number of connections between nodes i and j in H; $h^l_{S-(i,j)}$ and $h^l_{E-(i,j)}$ are the start time and end time of the l-th connection between nodes i and j in H, respectively. From the $h^*_{C-(i,j)}$ and $h^*_{D-(i,j)}$, the forwarding utility $V_{(i,j)}$ between nodes i and j in H can be calculated by:

$$V(i,j) = \frac{1}{H} \times \psi_A^{h^*_{D-(i,j)} - h^*_{U-(i,j)}} \tag{2}$$

where, ψA $\in$ [0, 1] is the aging constant. The weighted average between the forwarding utility V O-(i, j) in the current time window and that V N-(i, j) in the nearest time window is the mean forwarding utility V (i, j) of nodes i and j:

$$V(i,j) = \delta_W \times V_N(i,j) + (1 - \delta_W) \times V_O(i,j) \tag{3}$$

where, $\partial\delta_W \in [0, 1]$ is the weight constant. Formula (3) shows that the $V(i,j)$ between any two IoT nodes is positively correlated with the connection duration and the probability of next connection between the two nodes. Therefore, it is assumed that the forwarding utility $V(i,j)$ of nodes i and j is transmissible. As a result, nodes i and j not only update their forwarding utility $V(i,j)$ in each connection, but also update its own forwarding utility with any other node according to the forwarding utility between the other node and any other node. In other words, each of the two nodes update its own forwarding utility with any other node, whose forwarding utility with the other node is greater than the forwarding utility $V(i,j)$ between the two nodes.

Let $V(i,s)$ and $V(j,s)$ be the forwarding utilities between nodes i and s, and between nodes j and s, respectively; $\gamma_Z \in [0, 1]$ be the scaling constant of the transmissivity of forward utility. Then, the forwarding utility can be updated by:

$$V(i,s) = V_O(i,s) + \gamma_Z \times [V(i,s) - V_O(i,j)] \tag{4}$$

B. DESIGN OF INCENTIVE STRATEGY

Our incentive strategy for node communication consists of three parts: resources and attributes of IoT nodes, transaction rules, and message forwarding.

1) RESOURCES AND PROPERTIES OF IoT NODES

Under resource constraints, the IoT nodes in the universal HMM system include storage space, node energy, and virtual chip number. When an IoT node assists another node in message forwarding, the current storage space, node energy, and chip number are all viewed as the residual resources of the node. The three basic concepts were defined as follows to facilitate the description of residual storage space and residual energy of the IoT nodes.

The residual storage space of the i-th node was described by the percentage β_i of the residual cache of the node:

$$\beta_i = \frac{\beta_{gi}}{\beta_{M_i}} \times 100\% \tag{5}$$

where, β_{gi} and β_{Mi} are the residual caches of node i at the current moment and the initial moment, respectively. Let ε_{Mi} be the fixed initial energy of node i; ε_{Ri} be the residual energy of node i in assisting with message forwarding, i.e., the energy of the node at the current moment. Then, the percentage ε_i of residual energy of node i can be defined as the ratio of ε_{Ri} to ε_{Mi}:

$$\varepsilon_i = \frac{\varepsilon_{Ri}}{\varepsilon_{M_i}} \times 100\% \tag{6}$$

The greater the ε_i value, the more residual energy the node possesses to help with other nodes in message forwarding. At the beginning of communication, every IoT node in the system owns a certain number C_M of virtual chips used to request for assistance in message forwarding. During the communication, the residual virtual chip number of the IoT nodes changes dynamically, owing to their difference in the issuance and acceptance of such requests. Here, the residual virtual chip number is divided into three levels: I, II, and III. Let C_A and C_Q be the virtual chip number corresponding to the thresholds of levels I and III, respectively; $C_i(t)$ be the virtual chip number of node i at time t. Then, the level of

residual virtual chip number of node i can be determined by:

$$R_i = \begin{cases} \dfrac{C_i(t)}{C_A} & C_i(t) > C_A \ Level\ I \\ 1 & C_Q \le C_i(t) > C_A \ Level\ II \\ \dfrac{C_i(t)}{C_Q} & C_i(t) > C_Q \ Level\ III \end{cases} \tag{7}$$

If the residual virtual chip number $C_i(h)$ of node i at the current moment is greater than C_A, the node belongs to level I, i.e., the residual virtual chips are sufficient; if $C_i(h)$ is smaller than C_Q, the node belongs to level III, i.e., the residual virtual chips are insufficient; if $C_i(h)$ is between C_A and C_Q, the node belongs to level II, i.e., the residual virtual chip number is in equilibrium state. Depending on the levels of residual virtual chip number, the IoT nodes in the system have different willingness to assist with message forwarding.

2) TRANSACTION RULES

Suppose the sending node, intermediate node, and target node of a message are the i-th, j-th, and s-th node in the network, respectively. To assist in message forwarding of another node, node i firstly compares the forwarding utility $V(i, s)$ between nodes i and s with that $V(j, s)$ between nodes j and s. If $V(i, s)$ is smaller than $V(j, s)$, node i will request node j for forwarding; otherwise, node i will prioritize the sending of the next message. Then, node i as the request issuer and node j as the request accepter offer prices according to the pricing mechanism. The chip number offered by nodes i and j are noted as OP and AP_M, respectively. If OP is greater than AP_M, the forwarding request is successful, and node i will treat node j as satisfying the forwarding requirements. Finally, the sending node will choose a node with relatively low price among all the nodes that satisfy the forwarding requirements. If no node satisfies the requirements, the sending node will skip the current message and send the next message.

The residual storage space, message survival time, and node energy were assigned their respective weights α, τ, and θ to better characterize their impacts on the prices offered by the nodes. Let k_S be the size of the message from the sending node; β_i and ε_i be the percentage of residual cache and percentage of residual energy of the sending node, respectively; H_R and H_M be the initial survival time and residual survival time of the message, respectively. Then, the cost function of the pricing by the sending node can be defined as:

$$OP = k_S \times \left[\alpha(1-\beta_i) + \tau\left(1 - \frac{H_R}{H_M}\right) + \theta(1-\varepsilon_i)\right] \times \hat{R}_i \tag{8}$$

The level of residual chip number of the sending node can be calculated by:

$$\hat{R}_i = \begin{cases} R_i & Level\ I \\ 1 & Another\ level \end{cases} \tag{9}$$

During the communication, every IoT node might request for forwarding assistance, or receive such a request from another node. Therefore, the resources of every IoT node change constantly. As a result, the bidding willingness of each node, which is characterized by its storage space, energy, and virtual chip number, varies from moment to moment. To ensure the reasonability of the pricing mechanism, α, τ, and θ were determined by adaptive weighting method. Specifically, α, τ, and θ can be respectively defined by:

$$\alpha = \frac{(1-\beta_i)}{(1-\beta_i) + \left(1 - \frac{H_R}{H_{mM}}\right) + (1-\varepsilon_i)} \tag{10}$$

$$\tau = \frac{\left(1 - \frac{H_c}{H_M}\right)}{(1-\beta_i) + \left(1 - \frac{H_R}{H_M}\right) + (1-\varepsilon_i)} \tag{11}$$

$$\theta = \frac{\left(1 - \frac{\varepsilon_i}{H_M}\right)}{(1-\beta_i) + \left(1 - \frac{H_R}{H_M}\right) + (1-\varepsilon_i)} \tag{12}$$

Let k_M be the size of the message to be forwarded when the intermediate node offers assistance; β_i and ε_i be the percentage of residual cache and percentage of residual energy of the intermediate node, respectively. The pricing function of the assistance receiver can be defined as:

$$AP_R = k_M \times \left[\sigma\left(1-\beta_j\right) + \rho\left(1-\varepsilon_j\right)\right] \times \hat{R}_j \tag{13}$$

where, σ and ρ ($\sigma+\rho=1$) are the weight coefficients reflecting the situation of the residual cache and residual energy of the intermediate node at the current moment, respectively. The residual virtual chip number of the intermediate node can be obtained by:

$$\hat{R}_j = \begin{cases} R_j & Level\ III \\ 1 & Another\ level \end{cases} \tag{14}$$

The transaction price is $TP = 0.5 \times (OP + AP_M)$, when the forwarding request is successful. To characterize the probability for the sending node to successfully transmit a message to the target node at the cost of a unit of virtual chips, the cost performance of the delivery probability of the forwarding assistance task can be evaluated by:

$$CP = \frac{V(j, s)}{TP} \tag{15}$$

The greater the CP value, the more likely for the target node to successfully receive the message.

3) MESSAGE FORWARDING

Figure 2 illustrates the message forwarding flow under resource constraints.

III. DESIGN AND IMPLEMENTATION OF UNIVERSAL HMM SYSTEM

A. DENOISING

The universal HMM system receives signals that characterize human body health, including heart rate, electrocardiogram (ECG), blood oxygen, electromyogram (EMG), and trajectory, etc. The ECG could combine the results of chest computed tomography (CT), and nucleic acid test to support

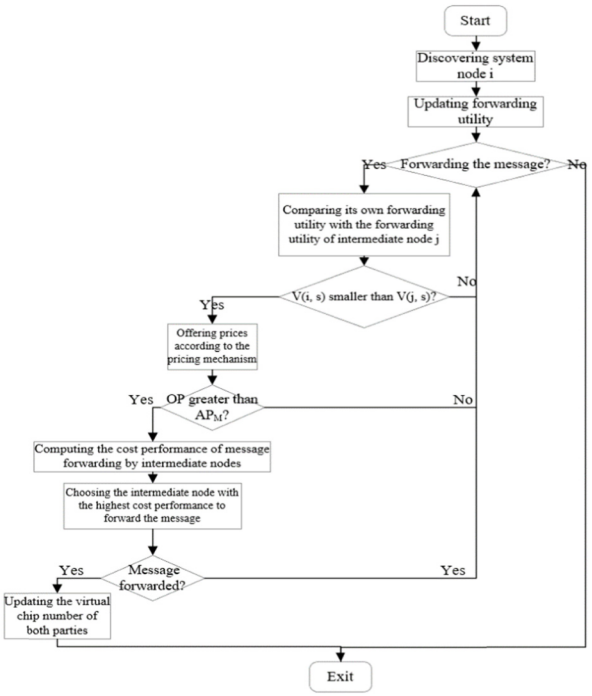

FIGURE 2. Message forwarding flow under resource constraints.

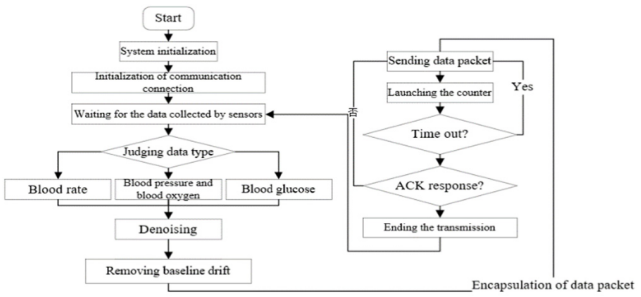

FIGURE 3. Workflow of information acquisition terminal.

the tracking of COVID-19 cases. These noises are more or less interfered by noises from 50Hz power supply frequency and baseline drift of 0.05-2Hz, or other random noises. Figure 3 presents the workflow of information acquisition terminal. It can be seen that this paper preprocesses the collected signals by denoising, thereby enhancing the accuracy of human physiological data.

Let $a(e)$, $RS(e)$, and $b(e)$ be the original input signal, reference signal, and actual output signal of the filter, respectively; $FA(e)$ be the adjustment coefficient of the adaptive filter. By the adaptive weighting method, the weight coefficient ω_A was adjusted and updated continuously according to the error signal fed back in the iterative process, such as to stabilize the error.

Let $a(e) = [a(e\text{-}1), a(e\text{-}2), \ldots\ldots, a(e\text{-}OF)]^T$, OF, and $\omega_A = [\omega_A^1, \omega_A^2, \ldots, \omega_A^M]^T$ be the input signal, order, and weighting vector of the adaptive filter, respectively. Then, the relationship between output signal $b(e)$ and the input signal $a(e)$ can be expressed as:

$$b(e) = \sum_{i=1}^{OF} \omega_A^i a(e-i) \tag{16}$$

The error signal can be obtained by:

$$FO(e) = RS(e) - b(e) \tag{17}$$

Combining formulas (16) and (17):

$$FA(e) = RS(e) - \sum_{i=1}^{OF} a(e-i) = RS(e) - a^T(e)\,\omega_A \tag{18}$$

Let λ be the step length. Then, the weighting vector ω_A can be adjusted and updated by:

$$\omega_A(e+1) = \omega_A(e) + 2\lambda FA(e)\,a(e) \tag{19}$$

λ can be replaced with a variable step length:

$$\lambda = 0.8\left\{1 - \frac{1}{FA^{|FA(e)|^{1.2}}}\right\} \tag{20}$$

In early iterations, λ changes significantly and converges quickly. With the growing number of iterations, λ changes less significantly, the algorithm has a small steady-state error, and the weight vector is optimal.

B. ELIMINATION OF BASELINE DRIFT

After denoising, the monitoring signal must be removed of baseline drift. This paper resorts to the sparse baseline estimation and denoising algorithm. Let I and O be the input and output of the algorithm, respectively; Δa be the data signal with positive sparsity; $I = \Delta a + O$ be the model of m-point input data I; η be the ratio of the asymmetric penalty function; W and E be banded convolution matrices; the elements in banded convolution matrix E be:

$$[e_i]_{m\times m} = \frac{1-\eta}{2} \tag{21}$$

μ_i be the regularization parameter. Then, the i-th order difference operator matrix can be expressed as:

$$DO = E^T E W^{-1} I - \mu_0 W^T e_i \tag{22}$$

Let $\Delta a = I$ be the initial value of iteration. Then, there exists a diagonal matrix:

$$[\Phi]_{m\times m} = \begin{cases} \dfrac{1+\eta}{4\,|\Delta a_m|}, & |\Delta a_m| \geq \varphi \\ \dfrac{1+\eta}{4\varphi}, & |\Delta a_m| \leq \varphi \end{cases} \tag{23}$$

Let ζ be the penalty function. Then, the $m\times m$ banded convolution matrix W can be expressed as:

$$[w_i]_{m\times m} = \frac{\zeta'(|DO\cdot\Delta a|_m)}{|DO\cdot\Delta a|_m} \tag{24}$$

The number of parameters can be calculated by:

$$N_C = 2\mu_0\Phi + \sum_{i=1}^{N_C} \mu_i DO^T \Phi_i DO \tag{25}$$

Suppose:

$$P = E^T E + W^T N_C W \tag{26}$$

Then,

$$\Delta A = WP^{-1}DO \tag{27}$$

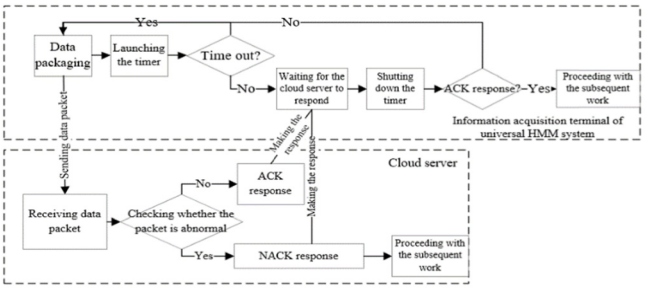

FIGURE 4. Workflow of synchronous communication.

Formulas (23)-(26) were repeated until the algorithm converges. The low-frequency baseline signal S_L can be expressed as:

$$S_L = I - \Delta a - EW^{-1}(I - \Delta a) \tag{28}$$

Then, the positive sparse signal Δa can be derived from the low-frequency baseline signal S_L.

C. FEATURE POINT DETECTION

This paper extracts and detects multiple feature points from the monitoring signal collected by the universal HMM system, including starting point, peak point, coincidence point, and valley point. To detect these points, the first-order difference algorithm was combined with sliding window to search for the local maximum or minimum of the signal. Let M_P be the data capacity of discrete monitoring signal $a[k]$. Then, the first-order difference result of the signal can be obtained by:

$$b[M_P - 1] = \left\{ \begin{array}{l} (a[1] - a[0]), (a[2] - a[1]) \\ \ldots\ldots, (a[M_D] - a[M_D - 1]) \end{array} \right\} \tag{29}$$

If the monitoring signal $b[k]$ after differential treatment is positive, the feature point of the signal is ascending; if it is negative, the feature point is descending. If $b[k] \times b[k+1]$ is smaller than zero, then the discrete monitoring signal $a[k]$ reaches an extreme at $i+1$; whether the extreme is maximum or minimum needs to be judged by comparing $b[k]$ with 0: if $b[k]$ is greater than zero, the extreme is maximum; if $b[k]$ is smaller than zero, the extreme is minimum.

D. SOFTWARE DESIGN OF COMMUNICATION PROTOCOL

The information acquisition terminal of the universal HMM system communicates with the cloud server in a synchronous manner. Before the communication, the system counter is given a fixed threshold. Once the terminal sends the collected data, the timer will start counting. If the cloud server does not respond when the count of the timer is above the threshold, the terminal will package the cached data, and resend them to the cloud server. If the cloud server makes an ACK response when the count is below the threshold, both the server and the terminal will continue with the subsequent data processing. If the monitoring data packet received by the server contain errors, the cloud server will make a NACK response; then, the terminal needs to repackage the cached data, and send them again to the server.

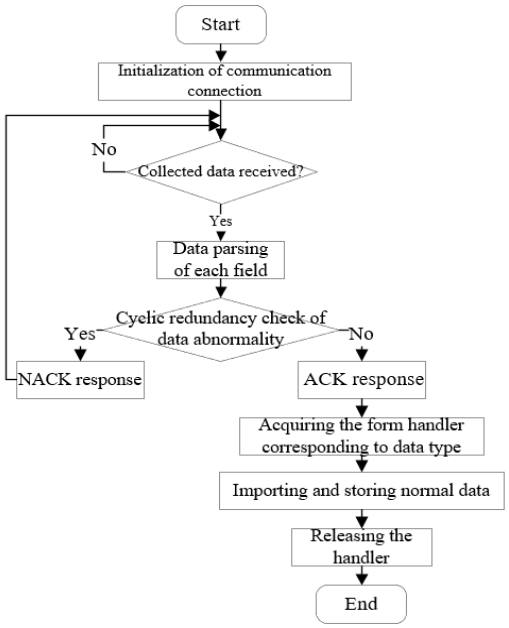

FIGURE 5. Workflow of cloud server.

TABLE 1. Blood glucose detection effect.

Reference value	Measured value							
	1	2	3	4	5	Mean	Standard error	Error rate
3.5	2.6	3.2	3.1	2.9	2.7	2.9	0.25	8.62%
6.3	5.7	5.2	5.6	6.3	6.1	5.78	0.43	7.43%
8.7	8.4	8.6	7.5	9.1	9.2	8.56	0.68	7.94%
10.5	10.9	10.2	12.1	12.5	12.6	11.66	1.05	9.01%
13.2	13.4	14.5	13.2	14.3	14.2	13.92	0.58	4.17%
15.6	16.2	17.1	13.9	17.5	18.3	16.6	1.69	10.18%
19.8	18.1	19.2	18.6	20.7	19.9	19.3	1.03	5.34%
22.3	21.5	22.4	21.7	21.6	22.5	21.94	0.47	2.14%
24.5	24.1	24.9	25.3	26.1	24.4	24.96	0.79	3.16%

E. WORKING PRINCIPLE OF CLOUD SERVER

Figure 5 shows the workflow of cloud server. It can be inferred that the cloud server mainly receives and parses the collected data transmitted by the naïve Bayes (NB)-IoT module, which integrates the client program of user datagram protocol (UDP). To improve its communication with the NB-IoT module, the cloud server must remain in sync with that module, and be able to realize the client program of UDP.

After setting up the communication connection with the information acquisition terminal, the cloud server can receive the collected data transmitted by every terminal. Then, the server will parse each field of the collected data, calculate the data frames by cyclic redundancy check algorithm, and compare the 2nd to 4th fields with the check data. If the two are equal, the server will make an ACK response; otherwise, it will make a NACK response. Upon obtaining the handler of the form corresponding to the data type, the cloud server will import the normal data into the corresponding form in the database for storage. After that, the handler will be released, marking the completion of data processing in the cloud server.

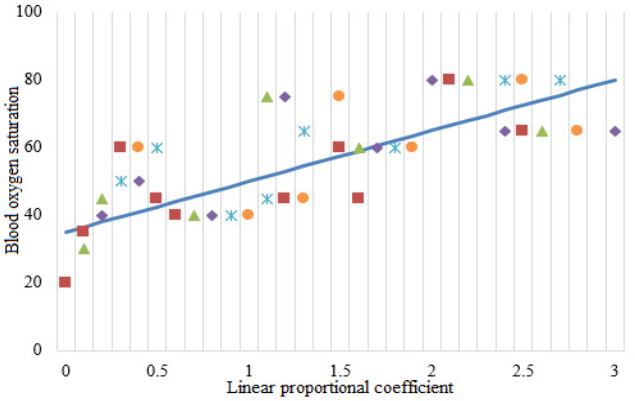

FIGURE 6. Variation of blood oxygen with linear proportional coefficient.

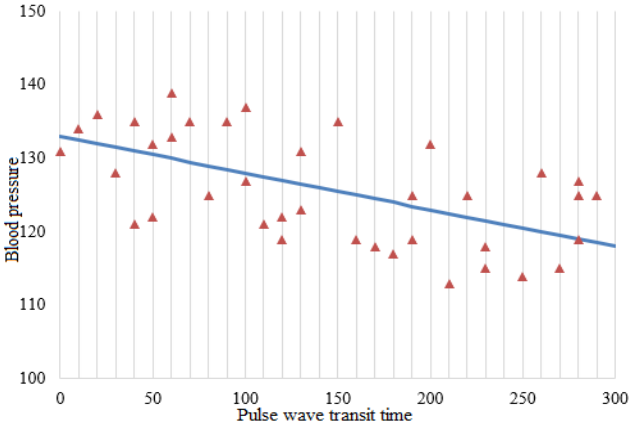

FIGURE 7. Variation of blood pressure with pulse wave transit time.

IV. EXPERIMENTS AND RESULTS ANALYSIS

Our universal HMM system adopts low-cost sensors to measure the signals that characterize human body health, including heart rate, ECG, blood oxygen, EMG, and trajectory. Therefore, the overall equipment has a high cost effectiveness. The product quality has been fully tested, indicating that the functions and operations of the system are harmless to the human body.

To verify the detection accuracy of our universal HMM system for blood glucose, the blood glucose detection module of the system was applied to measure blood glucose solutions with different concentrations. The data collected by our system were compared with the test results of a common blood glucose meter. As shown in Table 1, the measured values deviated from the reference values from the blood glucose meter by 10.18% at the maximum, which is smaller than the error standard of 15% specified by American Diabetes Association.

The blood oxygen detection module of our system was applied to measure the blood oxygen of five subjects, while changing the linear proportional coefficient. Then, the variation of blood oxygen with the coefficient was fitted into a curve, and the detection results were compared with the test results of a common smart bracelet (Figure 6). It can be seen that the blood oxygen, which was fitted from linear

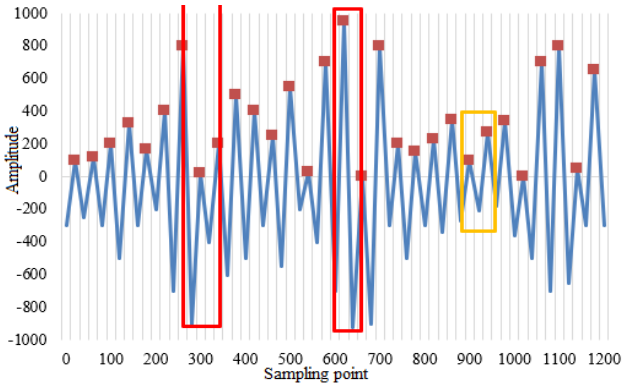

FIGURE 8. Test results on feature point detection.

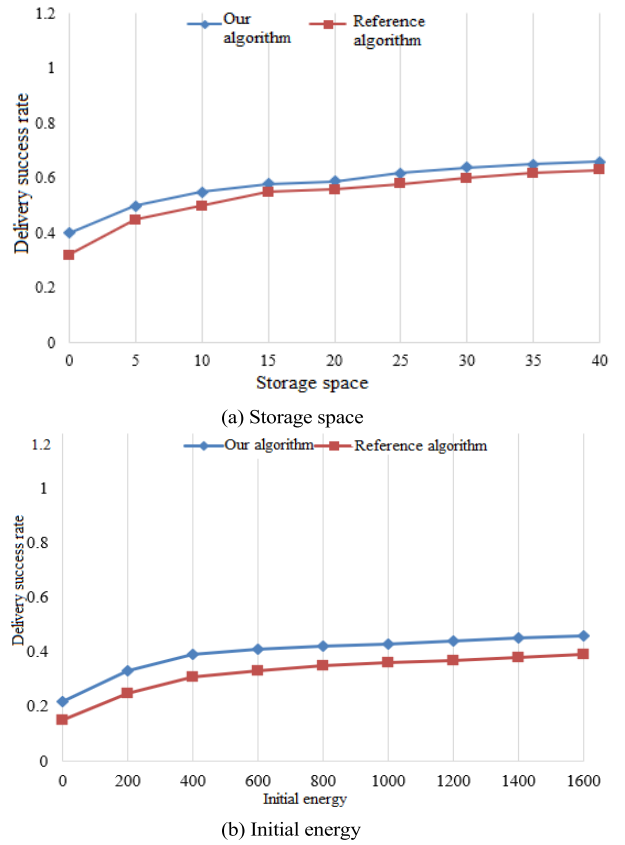

FIGURE 9. Relationship between node resources and success rate of data delivery.

proportional coefficient and blood oxygen saturation, was within ±3% of the results measured by the smart bracelet. Therefore, the algorithm in our system can effectively fit the blood oxygen.

Similarly, the variation of blood pressure measured by our system with pulse wave transit time was fitted by the least squares (LS) method (Figure 7). Obviously, the pulse wave transit time is negatively correlated with the systolic and diastolic blood pressures of human hearts. That is, the blood pressure of human body decreases with the extension of the pulse wave transit time.

Table 2 lists the heart rates of 9 subjects before and after strenuous exercise, which were measured by our universal

TABLE 2. Absolute error of heart rates before and after strenuous exercise.

Number	Error of measured result										Mean absolute error
	1	2	3	4	5	6	7	8	9	10	
1	2	3	5	1	3	2	4	5	2	1	2.8
2	2	3	5	4	5	2	4	1	2	3	3.1
3	3	3	2	3	1	4	4	2	1	2	2.5
4	1	4	1	2	1	2	5	1	4	3	2.4
5	4	2	3	5	3	2	2	3	2	2	2.8
6	2	3	2	3	2	1	3	2	2	3	2.3
7	3	5	1	2	4	3	2	1	4	1	2.6
8	2	4	1	3	2	2	1	3	2	2	2.2
9	1	5	3	2	4	2	2	1	5	4	2.9

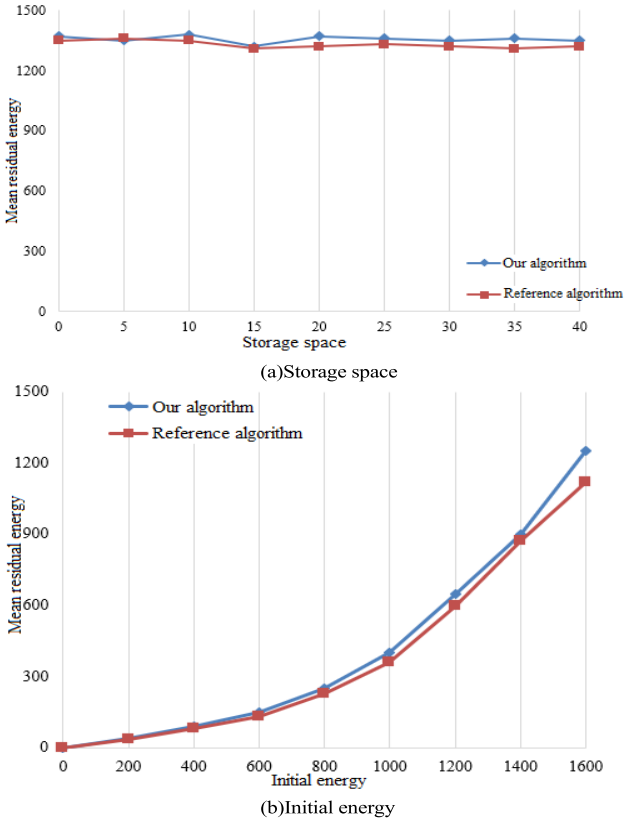

FIGURE 10. Relationship between node resources and mean residual energy.

HMM system. The errors between the measured data were calculated against the test results of a common smart bracelet. Each error is the average of ten groups of heart rate errors. As shown in Table 2, the heart rate error of the subjects was minimum before strenuous exercise, and relatively large after the exercise. This is consistent with the actual situation, calling for proper environment and conditions for heart rate detection by the universal HMM system.

The data collected by our system have cyclic features, and may change abruptly. Therefore, this paper takes the end point of a cycle as the start point of the next cycle, and designs a rectangular window with a width within $[T, 2T]$, where T is the width of the signal acquisition cycle. The peak and valley of the waveform can be identified by searching for the local maximum and minimum within the window.

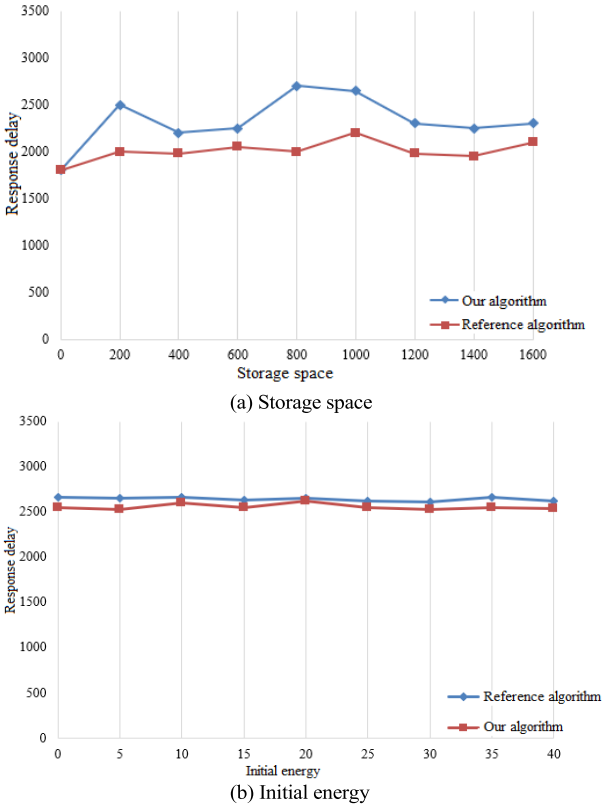

FIGURE 11. Relationship between node resources and response delay.

Figure 8 presents the test results on feature point detection of all collected data. The maximum and minimum feature points of local signals are marked in boxes.

Next, the performance of our algorithm was compared with that of broadcast incremental power algorithm (reference algorithm), as the IoT nodes underwent changes in storage space and initial energy: the storage space was changed from 0MB to 40MB at the step size of 5MB, and the initial energy was changed from 0J to 1,600J with a step size of 200J. Figure 9 presents the relationship between node resources and success rate of data delivery. For both algorithms, the success rate of data delivery increased with the storage space and initial energy of the IoT nodes. Comparatively, our algorithm achieved a much higher success rate than the reference algorithm, thanks to the additional step of choosing the most cost-effective intermediate nodes for message forwarding.

Figure 10 provides the relationship between node resources and mean residual energy. As shown in Figure 10(a), both our algorithm and the reference algorithm saw an increase in the mean residual energy with the growth of initial energy of the IoT nodes, but our algorithm had relatively high residual energy. This is because our algorithm selects the most cost-effective intermediate nodes for message forwarding, which means a message can arrive at the target node with fewer hops, without consuming too much initial energy of the nodes. As shown in Figure 10(b), the packet loss probability decreased with the expansion of storage space of the nodes. The mean residual energy of the nodes did not change

significantly, because both our algorithm and the reference algorithm are single-copy routing algorithms.

Figure 11 displays the relationship between system response delay and the storage space and initial energy of the IoT nodes. As shown in Figure 11(a), the system responses of the two algorithms both decreased with the growing initial energy of the nodes, and the system response of our algorithm was smaller than that of the reference algorithm. This is mainly because the pricing mechanism and residual energy of intermediate nodes of our algorithm suppress the delay of message forwarding induced by excessively fast energy consumption by active nodes.

V. CONCLUSION

This paper mainly explores the implementation of an IoT-based universal HMM system under resource-constrained environment. Firstly, the forwarding utility between adjacent IoT nodes was calculated, and an incentive strategy was designed for the IoT nodes under resource-constrained environment. Afterwards, a universal HMM system was designed, and data preprocessing was realized, including denoising, baseline drift removal, and feature point detection of the collected data. Further, the authors gave the design flow of system communication protocol and the work flow of cloud server. Experiments show that the detection modules of our system are effective in measurement, and provide the feature points detected on all collected data. Finally, our algorithm was proved superior than broadcast incremental power algorithm in terms of success rate of data delivery, mean residual energy of nodes, and system delay.

REFERENCES

[1] W. Hu, H. Li, W. Yao, and Y. Hu, "Energy optimization for WSN in ubiquitous power Internet of Things," *Int. J. Comput. Commun. Control*, vol. 14, no. 4, pp. 503–517, Aug. 2019.
[2] D. Chen, "Multiple linear regression of multi-class images in devices of Internet of Things," *Traitement du Signal*, vol. 37, no. 6, pp. 965–973, Dec. 2020.
[3] A. Rahaman, M. Islam, M. Islam, M. Sadi, and S. Nooruddin, "Developing IoT based smart health monitoring systems: A review," *Revue d'Intell. Artif.*, vol. 33, no. 6, pp. 435–440, Dec. 2019, doi: 10.18280/ria.330605.
[4] A. Gupta, C. Chakraborty, and B. Gupta, "Monitoring of epileptical patients using cloud-enabled health-IoT system," *Traitement du Signal*, vol. 36, no. 5, pp. 425–431, Nov. 2019.
[5] F. Ahamed, S. Shahrestani, and H. Cheung, "Internet of Things and machine learning for healthy ageing: Identifying the early signs of dementia," *Sensors*, vol. 20, no. 21, pp. 1–25, 2020.
[6] N. S. Kumar, G. Chandrasekaran, and K. P. Rajamanickam, "An integrated system for smart industrial monitoring system in the context of hazards based on the Internet of Things," *Int. J. Saf. Secur. Eng.*, vol. 11, no. 1, pp. 123–127, Feb. 2021.
[7] M. N. Khan and F. Naseer, "IoT based university garbage monitoring system for healthy environment for students," in *Proc. IEEE 14th Int. Conf. Semantic Comput. (ICSC)*, Feb. 2020, pp. 354–358.
[8] T. K. Brahmachary, S. Ahmed, and M. S. Mia, "Health, safety and quality management practices in construction sector: A case study," *J. Syst. Manage. Sci.*, vol. 8, no. 2, pp. 47–64, 2018.
[9] G. Cea, A. Gallego, M. T. Arredondo, and G. Fico, "Design of an evaluation tool to assess IoT solutions for active and healthy aging," in *Proc. 15th Medit. Conf. Med. Biol. Eng. Comput. (MEDICON)*, vol. 76, 2019, pp. 1038–1046.
[10] F. B. P. Prakasa, J. Maiga, and S. Suyoto, "IoT-based smart and healthy wardrobe system," in *Proc. Int. Conf. Artif. Intell. Inf. Technol. (ICAIIT)*, Mar. 2019, pp. 119–123.
[11] P. Das and B. M. Acharya, "Healthy environment using cloud IoT core," in *Proc. Int. Conf. Appl. Mach. Learn. (ICAML)*, May 2019, pp. 262–266.
[12] Y. Jia, B. Liu, W. Jiang, B. Wu, and C. Wang, "Poster: Enhancing remote healthiness attestation for constrained IoT devices," in *Proc. IEEE 28th Int. Conf. Netw. Protocols (ICNP)*, Oct. 2020, pp. 1–2.
[13] H. Wang and H. Zhou, "Research on precise layer healthy breeding based on Internet of Things," in *Proc. 7th Int. Conf. Informat., Environ., Energy Appl. (IEEA)*, 2018, pp. 227–230.
[14] A. M. Medrano-Gil, S. de los Ríos Pérez, G. Fico, J. B. M. Colomer, G. C. Sáncez, M. F. Cabrera-Umpierrez, and M. T. A. Waldmeyer, "Definition of technological solutions based on the Internet of Things and smart cities paradigms for active and healthy ageing through cocreation," *Wireless Commun. Mobile Comput.*, vol. 2018, pp. 1–15, Jan. 2018.
[15] H. Feng, Y. Wang, L. Qiao, and J. Zhu, "Internet of Thing system to extract hierarchical healthy and efficiency information for pump station optimization," in *Proc. 2nd Int. Conf. Big Data Internet Things*, 2018, pp. 162–166.
[16] J. Mitrpanont, W. Sawangphol, C. Chankong, A. Jitsuphap, and N. Wongkhumsin, "I-WISH: Integrated well-being IoT system for healthiness," in *Proc. 15th Int. Joint Conf. Comput. Sci. Softw. Eng. (JCSSE)*, Jul. 2018, pp. 1–6.
[17] M. Saelens, Y. Kinoo, and D. Weyns, "HeyCitI: Healthy cycling in a city using self-adaptive Internet-of-Thing," in *Proc. IEEE Int. Conf. Autonomic Comput. Self-Org. Syst. Companion (ACSOS-C)*, Aug. 2020, pp. 226–227.
[18] S. Vicini, S. Bellini, A. Rosi, and A. Sanna, "Well-being on the go: An IoT vending machine service for the promotion of healthy behaviors and lifestyles," in *Proc. Int. Conf. Des., User Exper., Usability*, in Lecture Notes in Computer Science: Including Subseries Lecture Notes in Artificial Intelligence and Lecture Notes in Bioinformatics, vol. 8014, 2013, pp. 594–603.
[19] T. Qiang, C. Wang, K. K. Adhikari, Q. Wu, and G.-H. Yang, "A design of microwave LC-resonator-based biosensor with double sensentive region for healthy-IoT applications," in *Proc. IEEE 2nd Int. Conf. Electron. Inf. Commun. Technol. (ICEICT)*, Jan. 2019, pp. 156–159.
[20] B. Gajsek, J. Marolt, B. Rupnik, T. Lerher, and M. Sternad, "Using maturity model and discrete-event simulation for industry 4.0 implementation," *Int. J. Simul. Model.*, vol. 18, no. 3, pp. 488–499, Sep. 2019.
[21] Y. Xiao, C. Li, L. Song, J. Yang, and J. Su, "A multidimensional information fusion-based matching decision method for manufacturing service resource," *IEEE Access*, vol. 9, pp. 39839–39851, 2021.
[22] E. I. Konstantinidis, A. S. Billis, L. Plotegher, G. Conti, and P. D. Bamidis, "Indoor location IoT analytics 'in the wild': Active and healthy ageing cases," in *Proc. XIV Medit. Conf. Med. Biol. Eng. Comput.*, in IFMBE Proceedings, vol. 57, 2016, pp. 1225–1230.
[23] U. Zuperl and F. Cus, "A cyber-physical system for smart fixture monitoring via clamping simulation," *Int. J. Simul. Model.*, vol. 18, no. 1, pp. 112–124, Mar. 2019.
[24] G. Marques and R. Pitarma, "Using IoT and social networks for enhanced healthy practices in buildings," in *Proc. Int. Conf. Eur. Middle East North Afr. Inf. Syst. Technol. Support Learn.*, in Smart Innov., Syst. Technol., vol. 111, 2019, pp. 424–432.

MIN ZHENG received the M.B.A. degree from Beijing Normal University, in 2014. He is currently pursuing the D.B.A. degree with Harbin University of Commerce. His research interest includes health management.

SHIZHEN BAI was born in October 1962. He currently serves as the Head of the School of Management, a Professor, and a Doctoral Tutor with Harbin University of Commerce. He is recognized as a Longjiang Scholar, a Young and Middle-Aged Expert of Heilongjiang Province, and the Famous College Teacher of Heilongjiang Province (Second Batch). His research interests include logistics and supply chain management.